



CHORUS

This is the accepted manuscript made available via CHORUS. The article has been published as:

Temperature-Dependent Fermi Surface Evolution in Heavy Fermion CeIrIn_5

Hong Chul Choi, B. I. Min, J. H. Shim, K. Haule, and G. Kotliar

Phys. Rev. Lett. **108**, 016402 — Published 5 January 2012

DOI: [10.1103/PhysRevLett.108.016402](https://doi.org/10.1103/PhysRevLett.108.016402)

Temperature-dependent Fermi surface evolution in heavy fermion CeIrIn₅

Hong Chul Choi,^{1,*} B. I. Min,¹ J. H. Shim,^{1,2,†} K. Haule,³ and G. Kotliar³

¹*Department of Physics, Pohang University of Science and Technology, Pohang 790-784, Korea*

²*Department of Chemistry, Pohang University of Science and Technology, Pohang 790-784, Korea*

³*Department of Physics, Rutgers University, Piscataway, NJ 08854, USA*

(Dated: November 21, 2011)

We have addressed theoretically the evolution of the heavy fermion Fermi surface (FS) as a function of temperature (T), using a first principles dynamical mean-field theory (DMFT) approach combined with density functional theory (DFT+DMFT). We focus on the archetypical heavy electrons in CeIrIn₅. Upon cooling, both the quantum oscillation frequencies and cyclotron masses show logarithmic scaling behavior ($\sim \ln(T_0/T)$) with different characteristic temperatures $T_0 = 130$ and 50 K, respectively. The enlargement of the electron FS's at low T is accompanied by topological changes around $T = 10 \sim 50$ K. The resistivity coherence peak observed at $T \simeq 50$ K is the result of the competition between the binding of incoherent $4f$ electrons to the spd conduction electrons at Fermi level (E_F) and the formation of coherent $4f$ electrons.

PACS numbers: 71.18.+y, 71.27.+a, 72.15.Qm

In Cerium-based heavy electron materials, the $4f$ electron's magnetic moments bind to the itinerant quasiparticles to form composite *heavy* quasiparticles at low temperature (T). The volume enclosed by the Fermi surface (FS) in the Brillouin zone incorporates the moments to produce a "large FS" due to the Luttinger theorem. When the f electrons are localized free moments, a "small FS" is induced since it contains only broad bands of conduction spd electrons. So, the FS volume is a sensitive probe of the character, localized or itinerant, of the heavy fermion system[1].

Intensive efforts have been devoted to the study of the quantum phase transition leading from a small to large FS at strictly zero temperature. While the FS, as a surface of discontinuity in the momentum distribution function, is sharply defined only at zero temperature, experimental probes such as the angle-resolved photoemission spectra (ARPES) and magnetic quantum oscillation experiments such as de Haas-van Alphen (dHvA) or Shubnikov-de Haas experiments identify the region of momentum space where zero energy fermionic excitations exist at finite temperature. ARPES experiment directly observes the FS in the momentum space. But, high resolution is required to determine the FS size. The quantum oscillation experiments measure the precise value of the FS area in a specific plane by probing the oscillation frequencies of magnetization as a function of the applied magnetic field. The quantum oscillation frequency(F), the so-called dHvA frequency, is proportional to the extremal cross-sectional area S_F of the FS ($F = \hbar S_F / 2\pi e$). The quantum oscillation experiments also provide the information on the cyclotron effective electron mass $m^* (= (\hbar^2 / 2\pi) \partial S_F / \partial \omega)$ and the geometry of the FS's.

The band structure calculation is a complementary tool to the quantum oscillation experiment to analyze the complicated FS of the multiple band system. Quan-

tum oscillation frequencies of heavy fermion materials, such as CeCu₆, UPt₃, and Ce(Ir,Co)In₅, are explained well by conventional band calculations because the itinerant $4f$ electrons behave as conduction electrons near E_F . Although the geometry and volume of FS's are well explained by the DFT band calculation, the detected cyclotron mass m^* is much larger than the corresponding DFT band mass m_b [2–5], because the DFT calculation can not describe the correlated $4f$ electronic states correctly. When the $4f$ electrons are localized in the antiferromagnetic (AFM) compounds, such as CeRhIn₅, CeIn₃, CeRh₂Si₂, the $4f$ -localized band model is more applicable to the description of the quantum oscillation experiments[2, 5]. The $4f$ -localized band model can be performed by treating the $4f$ electrons as core within the DFT (open-core DFT) band calculation[2], or by employing the DFT+ U band method (U : on-site Coulomb interaction)[7].

Ce T In₅ ($T = \text{Co, Rh, and Ir}$) has been a prototypical system to study the crossover behavior between the itinerant and localized $4f$ electrons. CeCoIn₅[8] and CeIrIn₅[9] have itinerant $4f$ electrons and superconducting ground states at low T . On the other hand, CeRhIn₅ has localized $4f$ electrons and the AFM ground state. The measured dHvA frequency of each compound identifies the nature of Ce $4f$ electrons, whether they are itinerant or localized. CeCoIn₅[2, 4, 6] and CeIrIn₅[2, 3] have enlarged electron FS's due to the contribution of itinerant $4f$ electrons, while CeRhIn₅ has similar geometry of FS's but smaller size of FS's[2, 5]. For CeRhIn₅, pressure-induced superconductivity was observed for $P > 1.63$ GPa[10], and the drastic change in the FS was detected at a critical pressure of $P_c \simeq 2.35$ GPa[11]. On the other hand, CeRh_{1-x}Co_xIn₅ shows the the doping-dependent reconstruction of FS deep inside the magnetically ordered state[12], away from the quantum critical point (QCP). The single-site DMFT is known to be a proper approach

for the description of finite temperature properties near the QCP. According to recent DMFT approaches[13], the single-site DMFT study gives a correct result well above a Neel order due to the suppression of the non-local correlation. The inter-site correlation becomes crucial only at extremely low T near the Neel ordering. Because CeIrIn₅ does not show the AFM ground state and the temperature in our calculation is usually well above the non-local fluctuation region, our DMFT study is still valid for the description of the system near the QCP. The T -dependent evolution between itinerant and localized electrons also has been described by the phenomenological two-fluid model, where the universal scaling behavior can be applied to various physical properties of the heavy fermion compounds[14–16].

In this Letter, we have addressed the T -dependent crossover from localized to itinerant $4f$ electrons in CeIrIn₅, and investigated its effects on the FS properties and electrical resistivity. The charge self-consistent version of DFT+DMFT approach[17], as implemented in Ref. [18], is based on the full-potential linearized augmented plane-wave (FP-LAPW) band method[19]. The correlated $4f$ electrons are treated dynamically by the DMFT local self-energy, while all other delocalized spd electrons are treated on the DFT level. The local self-energy matrix $\Sigma(\omega)$ is calculated from the corresponding impurity problem, in which full atomic interaction matrix is taken into account[20]. To solve the impurity problem, we used the vertex corrected one-crossing approximation (OCA)[17], and confirmed that the low T limit of the OCA is consistent with the continuous time quantum Monte-Carlo method[21, 22](The more information of the computational algorithm is given in the Supplementary).

The main difference between low and high T spectral functions in the DFT+DMFT calculation is the existence of $4f$ bands near E_F , as shown in Supplementary Fig. 2. Ce $4f$ bands at high T are absent near E_F , and their spectral weights are distributed into the lower and upper Hubbard bands. The spectral function near E_F can be well described by the quasiparticle band structures of other spd electrons although there is a small scattering rate due to the hybridization between the conduction electrons at E_F and the incoherent Ce $4f$ electrons in the Hubbard bands. As decreasing T , the spectral weight of the renormalized Ce $4f$ bands is increased continuously (see Supplementary Movie 1.). The hybridization of the $4f$ and other spd bands produces very massive almost flat quasiparticle band structures near E_F . These flat bands emerge as the narrow Kondo peak at E_F in the photoemission spectra[23].

The T -dependent FS has been extracted from the quasiparticle band structures. At low T , the FS's of the DFT+DMFT calculation are very similar to those of the DFT calculation, as shown in Fig. 1. Upon heating, the Ce $4f$ electrons become localized and their contribution to E_F is suppressed. Accordingly, the areas of electron

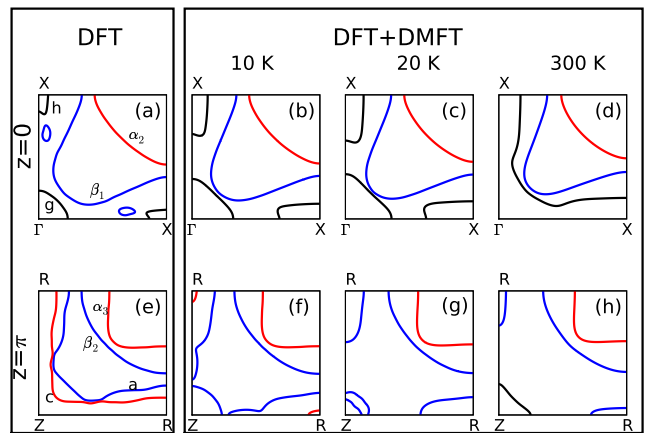


FIG. 1: (color online) The T -dependent FS evolution in the DFT+DMFT calculation. The FS's are extracted from the DFT+DMFT quasiparticle band structures at 10 K(b,f), 20 K(c,g) and 300 K(d,h). For comparison, the FS's obtained from the DFT band calculation are also provided (a,e). Because the main FS's in CeIrIn₅ are nearly cylindrical due to the quasi-2D nature of its crystal structure, the FS's only on the $z = 0$ and $z = \pi$ planes are shown. The FS's on these planes are identified from the dHvA frequencies because the symmetric plane provides the extremal cross-section of the FS. There are two main cylindrical electron FS's represented by α_i and β_i branches observed in the dHvA experiment (see (a) and (e)). Those branches are identified at all temperature range. On the other hand, the FS's denoted as g, h (hole FS's) and a, c (electron FS's) in the DFT calculation manifest topological changes with varying T in the DFT+DMFT calculation. Note that g, h, a, c branches were not identified clearly in the dHvA experiments. Color represents the different band index.

FS's (α_i and β_i) are continuously decreased. In contrast, there occur rather big changes in other FS's areas upon heating. The areas of the g and h hole FS's on the $z = 0$ plane grow and merge into one closed electron FS. The a electron FS identified at $T = 10$ K on the $z = \pi$ plane is divided at high T , and so new hole FS's appear near Z and R symmetry points. The continuous T -dependent evolution of the FS is provided in Supplementary Movie 2. By integrating the volume of electron FS's, the occupancy of the conduction electrons has been counted. It shows the continuous change from 3 to 4 electrons as temperature is decreased, which reflects the participation of one Ce $4f$ electron in the bonding.

Because the area of the FS is directly related to the size of the $4f$ electron contribution to E_F , we have investigated the T -dependent dHvA frequencies, as shown in Fig. 2(a). At high T , the dHvA frequencies are well consistent with those from the Ce $4f$ open-core DFT calculation. With decreasing T , they show the continuous increase with the participation of $4f$ electrons to E_F and follow the scaling behavior of $\ln(T_0/T)$, as shown in Fig. 2(c). All the branches show the same characteristic tem-

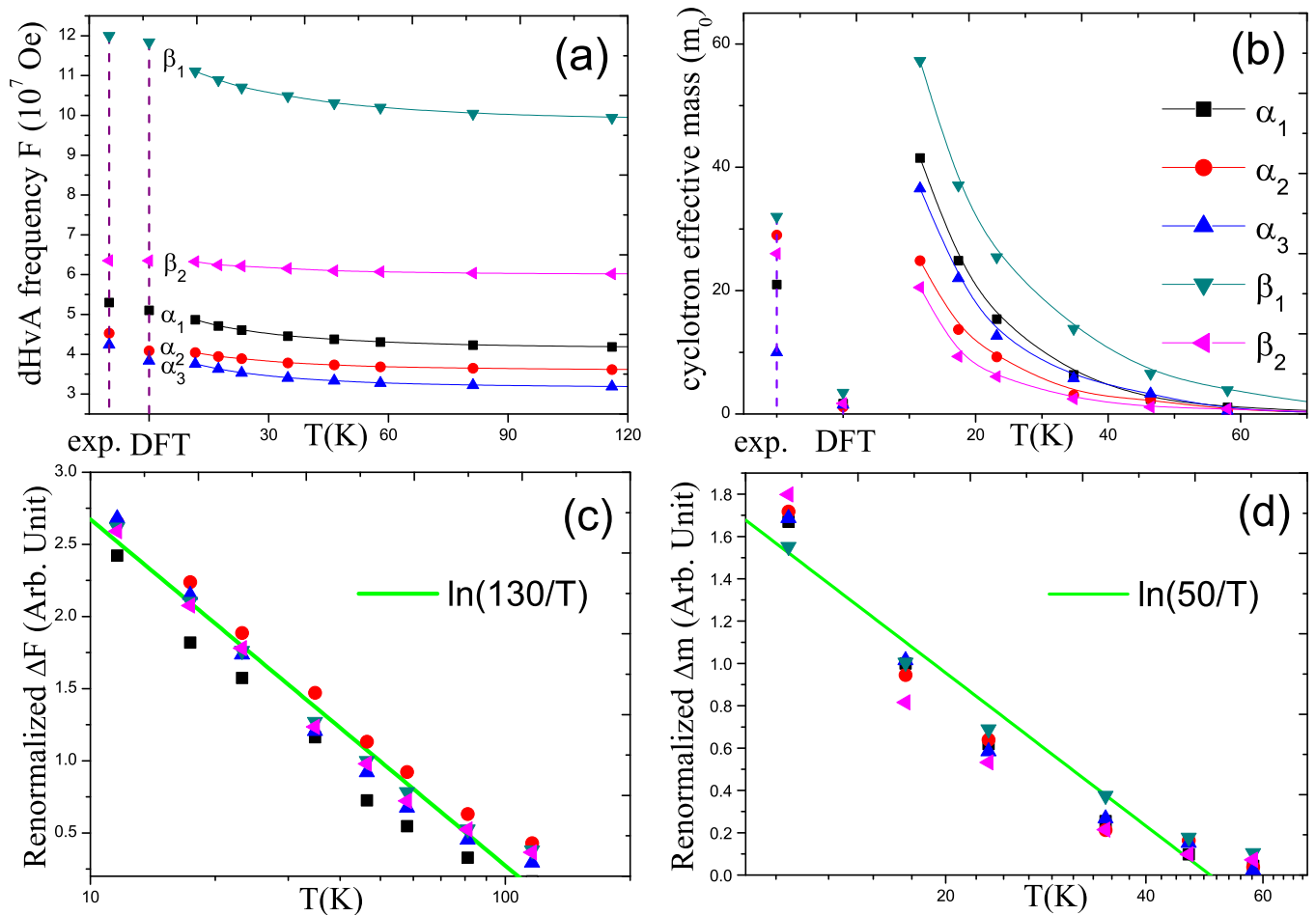


FIG. 2: (color online) The T -dependent dHvA frequencies (F) and cyclotron effective masses (m^*). The dHvA frequencies (a) and effective masses (b) of α_i and β_i branches are obtained from the DFT+DMFT method, and compared with those from the DFT method and experiments (exp). The corresponding FS's for each branch are provided in Fig. 1(a,e), except α_1 that corresponds to the maximum frequency among α_i branches and is located between the $z = 0$ and $z = \pi$ planes. At high T , the cyclotron masses are very small, ranging from 0.4 to 0.7 m_0 (m_0 : bare electron mass) for α_i and β_i branches. Such small cyclotron masses are also reproduced in the $4f$ open-core DFT calculation, in which only dispersive spd bands are crossing E_F . The low T dHvA frequencies from the DFT+DMFT method are consistent with the results of DFT method in which the $4f$ electrons are considered as itinerant type. (c) The renormalized ΔF_i of each branch shows the scaling behavior of $\ln(T_0^f/T)$ with the characteristic T of $T_0^f \sim 130$ K. (d) All the renormalized Δm^* 's show the similar scaling behavior, but with $T_0^m \sim 50$ K.

perature $T_0^f \sim 130$ K. This behavior is consistent with the increase of the number of conduction electrons with decreasing T .

The cyclotron mass corresponds to the effective mass of the carriers at the specific FS. As shown in Fig. 2(b) and (d), the calculated cyclotron masses also increase upon cooling, and follow a similar scaling behavior of $\sim \ln(T_0^m/T)$ with $T_0^m \sim 50$ K. The cyclotron masses are also well fitted with the two fluid model by Yang *et al.*[15]: $(1 - T/T_0)^{3/2}[1 + \ln(T_0/T)]$ with the same $T_0^m \sim 50$ K, as shown in the Supplementary Fig. 3. Interestingly, T_0^m is coincident with the coherent temperature T^* of Ce $4f$ states[23], but clearly different from T_0^f . This feature reveals the $4f$ electrons start to participate in

bonding through the hybridization with spd electrons at the temperature scale T_0^f , which is higher than the temperature T_0^m at which the coherent heavy fermion electronic states are formed. These results are reminiscent of recent experiment, which shows the occurrence of FS reconstruction much earlier than the quantum critical transition[12]. Note that the above scaling law is consistent with the two-fluid model[15], in which the coherent $4f$ bands start to grow below T^* .

All the calculated cyclotron masses at $T = 10$ K seem to be overestimated with respect to the experimental values[3] roughly by a factor of two. It is well known that the value of cyclotron mass has a substantial dependence on the applied magnetic field[4]. It is noted that

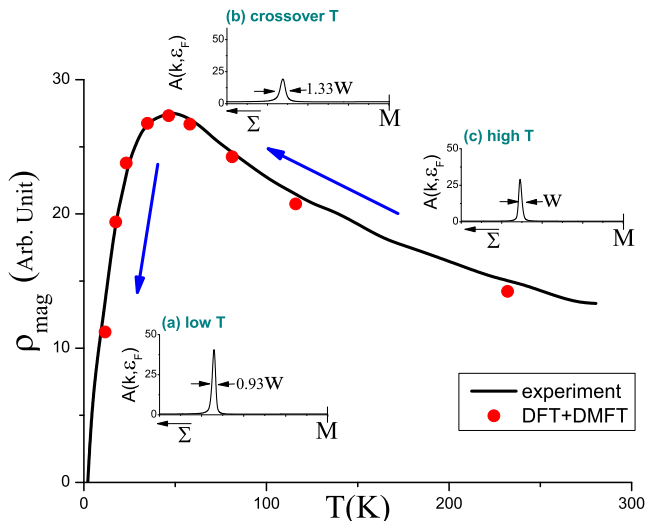


FIG. 3: (color online) The magnetic part ($4f$ electron contribution) of the resistivity as a function of T . The experimental electrical resistivity is obtained by subtracting the resistivity of LaIrIn_5 from that of CeIrIn_5 [5]. Inset Fig. (a), (b), and (c) show the broadening changes of spectral weights at E_F at low (10K), crossover (50 K), and high temperature (1000 K), respectively. Σ means the direction from M to Γ in momentum space.

the suppression of the m^* with increasing magnetic field was studied by the spin-dependent mass[24–27], or the Zeeman effect[28, 29].

The continuous change of FS properties with T variation is deeply related to the transport properties. Figure 3 provides the calculated resistivity for CeIrIn_5 as a function of T , which is compared to the experimental electrical resistivity. The electrical resistivity is calculated using the real part of the dc conductivity (σ)[18] based on the DFT+DMFT spectral function near E_F :

$$\sigma^{\mu\nu} = \frac{\pi e^2}{V} \sum_{\mathbf{k}} \int d\omega \left(-\frac{df}{d\omega} \right) \text{Tr} [A(\mathbf{k}, \omega) v^{\mathbf{k}\mu} A(\mathbf{k}, \omega) v^{\mathbf{k}\nu}].$$

Here μ and ν represent spatial coordinates. V , $f(\omega)$, and v are the primitive volume, the Fermi Dirac distribution function, and the velocity, respectively. The calculated resistivities from low to high T are in good agreement with the experimental resistivity. At high T , the electronic carriers from dispersive spd bands become more and more decoupled from localized electrons in the $4f$ shell, hence the carriers are scattered less at very high T . Upon cooling, the hybridization among local moments and spd carriers increases while the $4f$ electrons remain very incoherent above 50 K, causing enhanced scattering mechanism for electric carriers. Below the scale T_0^m , the electrons in the $4f$ shell also gain coherence which substantially suppresses the resistivity. Therefore, the maximum resistivity is observed near 50 K. Inset Fig. 3(a), (b), and (c) show the broadening of spectral weight at E_F , calculated at low, crossover, and high T , respectively. The broadening corresponds to the scattering rate

at the specific \mathbf{k} -point. It is noted that the spreading of the spectral weight at crossover is wider than that at high or low T . This finding confirms that the DFT+DMFT calculation describes well the crossover behavior of Ce $4f$ electrons with one T_0^f (~ 130 K) for the participation of $4f$ electrons in the conduction and another T_0^m (~ 50 K) for the formation of coherent heavy electron $4f$ bands. The increase of the scattering rate approaching T_0^m from high T can be comprehended by the local Kondo effect scaled by T_0^f . The decrease from the maximum scattering rate with lowering T is understood by the lattice coherence, which is consistent with the meaning of T_0^m .

We have examined the evolution of the heavy fermion state using electronic structure methods. As in the two fluid phenomenology[14], the experimental studies of other heavy fermion systems[30] as well as the slave boson studies[31, 32], the crossover from the high T regime, where moments and quasiparticles coexist, to the low T Fermi liquid heavy fermion state, has a rich structure characterized by multiple energy scales. We have found that it is characterized by multiple scales which have a clear correspondence with physical observables. T_0^f is the onset of the sharp crossover where the small FS begins distorting towards the low T FS. At a lower T_0^m , composite quasiparticles formed from f -moments and conduction electrons emerge, and this is signaled by a maximum of the resistivity. By that point, the FS has reached a shape which is closer to its zero temperature final value, but the material is not yet a Fermi liquid, which is only reached at a much lower temperature T_{FL} . We can only put bounds for this quantity as being lower than 10 K for the 115 material.

The theory can be tested using several techniques such as ARPES, Compton scattering and scanning tunnelling microscopy, which have been developed as powerful tools for exploring the evolution of the electronic structure and are currently under way[33]. Our theory predicts that both T_0^m and T_0^f increase as a function of pressure in the CeIrIn_5 material. More generally, it would be interesting to follow these scales as a function of control parameters such as pressure and composition, to investigate the behavior of T_0^m and T_0^f in related materials which can be driven to a QCP.

We acknowledge useful discussions with Tuson Park. This work was supported by the NRF (No. 2009-0079947, 2010-0006484, 2010-0026762), WCU through KOSEF (No. R32-2008-000-10180-0), and by the POSTECH BK21 Physics Division. K. Haule was supported by Grant NSF NFS DMR-0746395 and Alfred P. Sloan fellowship. G. Kotliar was supported by NSF DMR-0906943

* Electronic address: ithink@postech.ac.kr

† Email of corresponding author: jhshim@postech.ac.kr

- [1] R. Settai *et al.*, *J. Phys. Soc. Jpn.* **76**, 051003 (2007).
- [2] S. Elgazzar *et al.*, *Phys. Rev. B* **69**, 214510 (2004).
- [3] Y. Haga *et al.* *Phys. Rev. B* **63**, 060503(R) (2001).
- [4] R. Settai *et al.*, *J. Phys.: Condens. Matter* **13**, L627 (2001).
- [5] H. Shishido *et al.*, *J. Phys. Soc. Jpn.* **71**, 162 (2002).
- [6] D. Hall *et al.*, *Phys. Rev. B* **64**, 212508 (2001).
- [7] J. L. Wang *et al.*, *J. Appl. Phys.* **93**, 6891 (2003).
- [8] C. Petrovic *et al.*, *J. Phys. Cond. Matt.* **13**, L337 (2001).
- [9] C. Petrovic *et al.*, *Europhys. Lett.* **53**, 354 (2001).
- [10] H. Hegger *et al.*, *Phys. Rev. Lett.* **84**, 4986 (2000).
- [11] H. Shishido *et al.*, *Phys. Soc. Jpn.* **74**, 1103 (2005).
- [12] S. K. Goh *et al.*, *Phys. Rev. Lett.* **101**, 056402 (2008).
- [13] D. Tanasković *et al.*, *Phys. Rev. B* **84**, 115105 (2011).
- [14] S. Nakatsuji *et al.*, *Phys. Rev. Lett.* **92**, 016401 (2004).
- [15] Y.-f. Yang *et al.*, *Phys. Rev. Lett.* **100**, 096404 (2008).
- [16] Y.-f. Yang *et al.*, *Nature* **454**, 611 (2008).
- [17] G. Kotliar *et al.*, *Rev. Mod. Phys.* **78**, 865 (2006).
- [18] K. Haule *et al.*, *Phys. Rev. B* **81**, 195107 (2010).
- [19] P. Blaha *et al.* in *Wien2K*, edited by K. Schwarz (Technische Universität Wien, Austria, 2001).
- [20] R. D. Cowan, *The Theory of Atomic Structure and Spectra* (Univ. California Press, Berkeley, 1981).
- [21] K. Haule, *Phys. Rev. B* **75**, 155113 (2007).
- [22] P. Werner *et al.*, *Phys. Rev. Lett.* **97**, 076405 (2006).
- [23] J. H. Shim *et al.*, *Science* **318**, 1615 (2007).
- [24] J. Spalek *et al.*, *Phys. Rev. Lett.* **64**, 2823 (1990).
- [25] P. Korbel *et al.*, *Phys. Rev. B* **52**, R2213 (1995).
- [26] J. Bauer *et al.*, *Phys. Rev. B* **76**, 035118 (2007).
- [27] S. Onari *et al.*, *J. Phys. Soc. Jpn.* **77**, 023703 (2008).
- [28] A. Wasserman *et al.*, *J. Phys.: Condens. Matter* **1**, 2669 (1989).
- [29] T. Ebihara *et al.*, *Phys. Rev. Lett.* **90**, 166404 (2003).
- [30] P. Gegenwart *et al.*, *Science* **315**, 969 (2007).
- [31] S. Burdin *et al.*, *Phys. Rev. B* **79**, 115139 (2009).
- [32] S. Burdin *et al.*, *Phys. Rev. Lett.* **85**, 1048 (2000).
- [33] J. D. Delinger *et al.*, private communications.